Chemistry & Biology, Vol. 12, 1103–1115, October, 2005, ©2005 Elsevier Ltd All rights reserved. DOI 10.1016/j.chembiol.2005.08.008

A Proteome-Wide CDK/CRK-Specific Kinase Inhibitor Promotes Tumor Cell Death in the Absence of Cell Cycle Progression

Maureen Caligiuri,[1,3] Frank Becker,[2,3]
Krishna Murthi,[1] Faith Kaplan,[1] Severine Dedier,[2]
Christine Kaufmann,[2] Andy Machl,[1]
Gabriele Zybarth,[1] Judson Richard,[1] Nick Bockovich,[1]
Art Kluge,[1] and Nikolai Kley[1,2,*]
[1]GPC Biotech, Inc.
610 Lincoln Street
Waltham, Massachusetts 02451
[2]GPC Biotech AG
Fraunhoferstrasse 20
82152 Martinsried
Germany

Summary

The identification of molecular determinants of tumor cell survival is an important objective in cancer research. Here, we describe a small-molecule kinase inhibitor (RGB-286147), which, besides inhibiting tumor cell cycle progression, exhibits potent cytotoxic activity toward noncycling tumor cells, but not nontransformed quiescent fibroblasts. Extensive yeast three-hybrid (Y3H)-based proteome/kinome scanning with chemical dimerizers revealed CDK1/2/3/5/7/9 and the less well-characterized CDK-related kinases (CRKs) p42/CCRK, PCTK1/3, and PFTK1 as its predominant targets. Thus, RGB-286147 is a proteome-wide CDK/CRK-specific kinase inhibitor whose further study could yield new insight into molecular determinants of tumor cell survival. Our results also suggest that the [1, 3, 6]-tri-substituted-pyrazolo[3,4-d]-pyrimidine-4-one kinase inhibitor scaffold is a promising template for the rational design of kinase inhibitors with potential applications to disease indications other than cancer, such as neurodegeneration, cardiac hypertrophic growth, and AIDS.

Introduction

Cyclin-dependent kinases (CDKs) play many important roles in cell cycle control, transcription, and the regulation of cellular proliferation, apoptosis, and differentiation (for reviews, see [1–4]). They exist as multiprotein complexes, the core components being a catalytic subunit (the kinase) and a regulatory subunit (the cyclin or other regulatory protein). CDKs are active only in association with these regulatory partners. Besides the cyclins, additional regulatory subunits and protein kinases may modulate CDK activity, substrate recognition, and/or subcellular localization. For instance, various CDK-inhibitory subunits (CKIs), such as $p21^{Cip1}$/WAF1, $p15^{INK4b}$, $p16^{INK4a}$, $p27^{Kip1}$, and p57, regulate the activities of CDK/cyclin complexes and can provide tissue-specific mechanisms by which their function is regulated in response to extracellular and intracellular signals. Activation of CDKs is also regulated via post-translational modifications by various kinases and phosphatases [5, 6]. These include CDK-activating kinases (CAKs) such as CDK7 and p42/CCRK [7], the inhibitory kinases WEE1 and Myt1 [8], and the CDC25A,B,C phosphatases.

Some of the known CDKs play a role in the regulation of the cell cycle machinery, and they control cell cycle progression at multiple stages of the cell cycle [1, 9]. The key cell cycle CDKs are CDK1 (CDC2), CDK2, and CDK4/6. CDK1/cyclin B (a.k.a. mitosis promoting factor, MPF) plays an important role in G2/M cell cycle transition, CDK4/6-D-type cyclin complexes play important roles in integrating extracellular signals and promoting an orderly progression through the G1 phase, and CDK2/cyclin E or A play important roles in G1/S transition and S phase. Recent studies indicate that in certain settings CDK2 and CDK4/6 display a relative functional redundancy with respect to regulation of Rb phosphorylation and regulation of G1/S phase transition [9]. For example, CDK4/6 appears to be able to compensate for the lack of CDK2 expression/activity in cultured embryonic fibroblast cells and colon cancer cells [10, 11]. These findings have led to the hypothesis that CDK2 may not be a suitable target for the development of anticancer agents. This conflicts with previously held conjectures that CDK2 plays an essential role in cell cycle progression and survival of transformed cells [12, 13]. On the other hand, proliferation of melanoma cells has most recently been reported to exhibit CDK2 dependence [14], suggesting that chemical inhibition of CDK2 may have therapeutic benefit in the treatment of malignant melanoma. Alternative functional properties of CDKs, which are unrelated to cell cycle regulation, include: induction of apoptosis in various cell types (CDK1, CDK2) [15], induction of neuronal cell death (CDK5) [3, 16], regulation of HIV1 replication (CDK9) [17, 18], and cardiac hypertrophic growth (CDK9) [19, 20].

An understanding of the role of CDKs in the pathogenesis of various diseases has stimulated an intensive search for selective pharmacological inhibitors of these kinases. Compounds of various chemotypes have been described in recent years [3, 4]. Most of these low molecular weight kinase inhibitors interact with the nucleotide binding pocket of the catalytic domain of these enzymes, thereby effectively inhibiting catalysis and substrate phosphorylation. However, due to the structural similarity of kinase domains, these molecules can also exhibit significant crossreactivity with other kinases [4, 21], as well as with other classes of purine binding proteins [22]. Similar observations have been reported for other classes of kinase inhibitors. For example, Cohen and colleagues recently showed that many kinase inhibitors, when profiled against a larger set of kinases, are less selective than previously recognized [23, 24]. Chemical proteomics studies reported similar findings for various serine/threonine and tyrosine kinase inhibitors [21, 22, 25–30]. Thus, especially

*Correspondence: nikolai.kley@gpc-biotech.com
[3]These authors contributed equally to this work.

A

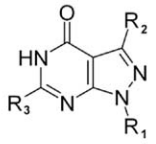

B

ID	R1	R2	R3		CDK1/B	CDK2/E	CDK4/D1	CDK6/D3	HCT116	
Flavopiridol					0.485	1.340	0.155	0.663*	0.221	
RGB-286147				IC50 [μM]	0.048	0.015	0.839	0.282	0.051	IC50 [μM]
RGB-285940					0.230	0.007	0.858	nd	0.410	
RGB-286331					0.043	0.004	nd	nd	0.220	
RGB-285960					0.310	0.009	1.750	nd	0.064	
RGB-310596				% inhibition at 0.1 μM/1 μM	0/6	17/15	nd	0/0	>10	
RGB-310595	H				0/0	8/28	nd	3/0	>10	
RGB-310590		H			29/88	69/97	nd	4/43	5.5	
RGB-310591					0/0	2/3	nd	0/0	>10	

C

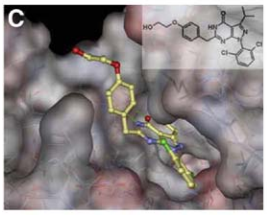

Figure 1. Chemical Structures and Activity Profiles of Pyrazolopyrimidone Analogs

(A) Core structure of the [1, 3, 6]-tri-substituted-pyrazolo[3,4-d]-pyrimidine-4-one kinase inhibitor scaffold.

(B) Structure-activity profiles of pyrazolopyrimidone analogs. IC_{50} values for inhibition of in vitro kinase activity of purified CDKs were determined, as indicated (an asterisk indicates that flavopiridol was tested against the CDK6/D2 complex.). Alternatively, percent inhibition of kinase activity at 0.1 μM and 1 μM compound were determined, as indicated. Inhibition of HCT116 cell proliferation after 72 hr of incubation with compounds was determined by using the SRB assay.

(C) A model for binding of RGB-286147 in the ATP binding site of CDK2. Hydrogen bonds to the hinge region (Leu83) are shown as green lines, the surface is colored by atom charges. The terminal hydroxy group clearly points toward solvent, suggesting a suitable site for coupling of a PEG spacer for the synthesis of methotrexate fusion compounds (MFCs, see Figure 4).

given the size of the human kinome (>500 kinases) [31], comprehensive target profiling of kinase inhibitors remains a critical issue when evaluating or validating their mode of action (MoA), their suitability as molecular probes, and their therapeutic potential. Driven by the need for comprehensive small-molecule target identification screening capabilities, chemical proteomics initiatives have seen the emergence of various alternatives to classical in vitro enzyme screening assays for inhibitor profiling (for reviews, see [22, 32–37]). We recently described a yeast three-hybrid system (Y3H) for the analysis of small molecule-protein interactions in intact cells, as well as its application to proteome-wide screening for cellular targets of kinase inhibitors [21, 37]. Using this approach, we have begun to systematically scan the proteome for targets of a number of kinase inhibitors.

In this study, we used this approach to evaluate the MoA of small molecules that are based on a [1, 3, 6]-tri-substituted-pyrazolo[3,4-d]-pyrimidine-4-one kinase inhibitor scaffold. Compounds of this chemical class were recently described by colleagues at Bristol Myers-Squibb and our laboratory [38]. They were shown to be inhibitors of the cell cycle kinases CDK1 and CDK2 (and sometimes CDK4), and to exhibit potent antiproliferative activity. Here, we show for a member of this chemical class that it not only inhibits the proliferation of many types of tumor cells, but that it also exhibits potent cytotoxic activity toward HCT116 colon cancer cells, irrespective of whether they are actively engaged in cell cycle progression or not. We also find that RGB-286147 targets kinases other than CDK1/2, although it embodies a CDK/CRK-specific kinase inhibitor with an apparent narrow target spectrum. We conclude that RGB-286147 is a molecular probe suitable for investigating molecular determinants of tumor cell survival and that the [1, 3, 6]-tri-substituted-pyrazolo[3,4-d]-pyrimidine-4-one kinase inhibitor scaffold provides a heretofore unrecognized template for the rational design of kinase inhibitors with potentially diverse therapeutic applications.

Results

CDK Inhibition and Antiproliferative Activity of [1, 3, 6]-tri-substituted-pyrazolo[3,4-d]-pyrimidine-4-one

Figures 1A and 1B summarize the chemical structures of [1, 3, 6]-tri-substituted-pyrazolo[3,4-d]-pyrimidine-4-one analogs used in this study; their effects on the in vitro kinase activity of CDK1, CDK2, and CDK4/6; and their antiproliferative activities toward HCT116 colon cancer cells. HCT116 cells express wild-type p53 and Rb proteins. They also express high levels of cell cycle CDK/cyclin proteins, posing a challenge to inhibitors of this class of kinases. Analysis of the activities of these compounds (and various related compounds; data not shown) suggests that the presence of a 2,6-disubstituted aryl group at position 1 of the [1, 3, 6]-tri-substituted-pyrazolo[3,4-d]-pyrimidine-4-one scaffold, combined with a small lipophilic group at position 3 and a benzyl substituent at position 6, are important for potent CDK1/2-inhibitory activity and HCT116-antiproliferative activity. The presence at position 1 of an unsubstituted phenyl group (RGB-310596) or no substituent (RGB-310595) resulted in a major loss in CDK1/2-inhibitory activity, as well as antiproliferative activity. Similarly, the presence at position 3 of a bulky substituent (RGB-310591) or no substituent (RGB-310590) resulted in a decrease in enzyme-inhibitory activity as well as cellular activity. Analogs with various substituents at the para position of the R3 benzyl group generally retained potent CDK2-inhibitory and HCT116-antiproliferative activity. Somewhat variable effects were observed with respect to CDK1-inhibitory activity (e.g., compare RGB-286147 and RGB-286331 with

A

		RGB-286147		Flavopiridol	
Inhibitor [nM]		50	100	50	100
		% inhibition of BrdU incorporation			
Time	24h	83	92	12	34
	48h	77	97	10	18

C

	inhibition of viability: IC50 [μM]	
	HCT116	IMR90
RGB-286147 Calcein AM assay (72h)	0.025	0.009
RGB-286147 Clonogenic assay (24h)	0.057	nd
Flavopiridol Clonogenic assay (24h)	0.250	nd

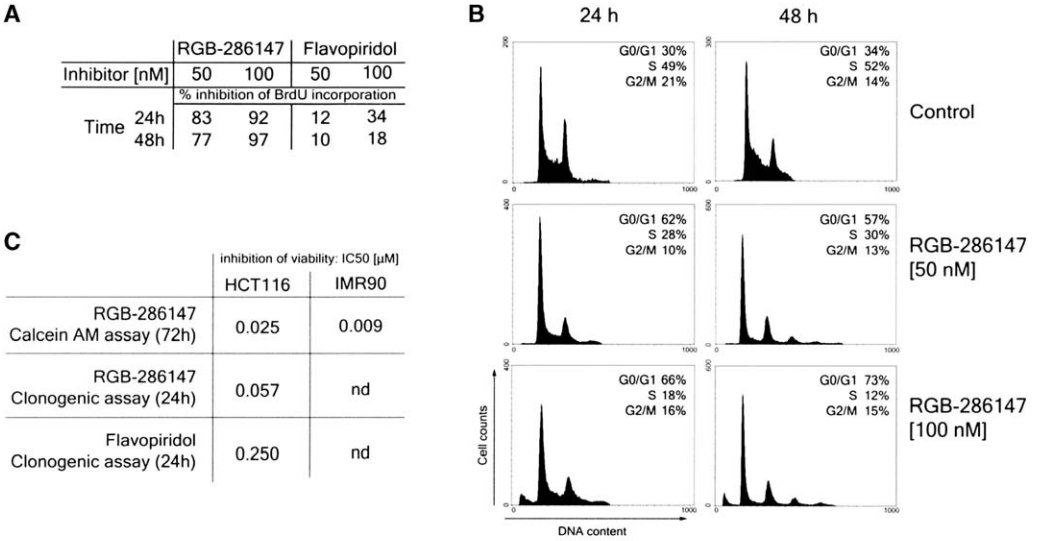

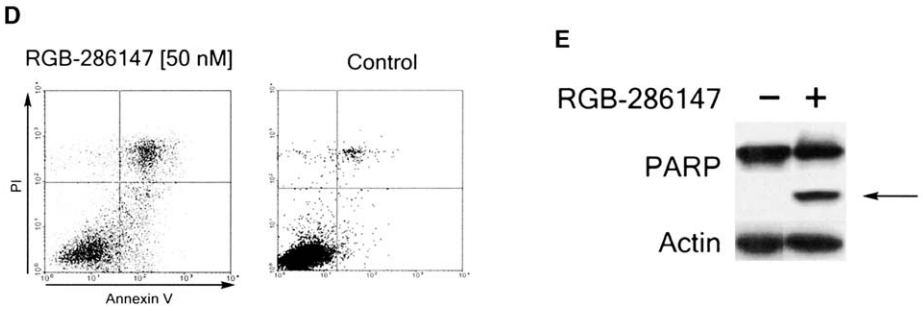

Figure 2. RGB-286147 Inhibits Cell Cycle Progression and Promotes Apoptosis

(A) RGB-286147 inhibits DNA replication, as determined by a BrdU incorporation assay.

(B) Cell cycle analysis. Cells were incubated with RGB-286147, as indicated. Control cells were treated with DMSO. Representative cell cycle profiles are shown, with the corresponding quantifications of the percent of cells in the different phases of the cell cycle.

(C) Effects of RGB-286147 on viability of asynchronously growing HCT116 and IMR90 cells, as determined by using a Calcein AM assay (72 hr incubation) or a clonogenic assay (24 hr drug exposure).

(D) Exposure to RGB-286147 promotes emergence of annexin-V-positive, PI-negative HCT116 cells (lower right quadrant) compared to DMSO-treated control cells.

(E) Proteolytic cleavage of poly-ADP-ribose-polymerase (PARP) after incubation of HCT116 cells with 100 nM RGB-286147 for 48 hr.

RGB-285960). CDK1/2 active compounds were generally significantly less active against CDK4/6 (e.g., RGB-286147). Data for flavopiridol, a known nonselective CDK inhibitor [4], are included for comparison. In summary, significant HCT116-antiproliferative activity was observed with compounds that also exhibited CDK1/2-inhibitory activity. However, CDK2 is not essential for HCT116 cells to undergo mitosis [11]. Furthermore, no tight correlation between inhibition of CDK1 in vitro and inhibition of HCT116 proliferation was observed, suggesting that mechanisms other than CDK1/2 inhibition might be involved in the antiproliferative activity of these compounds. These observations provided the impetus to examine in more detail the cellular activity profile of one such compound, RGB-286147, and its potential target spectrum. Figure 1C shows a model for binding of RGB-286147 to the active site of CDK2. The hypothesized mechanism of enzyme inhibition is consistent with an ATP-competitive mode of action, as previously suggested for related analogs [38].

Cellular Activity Profile of RGB-286147: Cell Cycle Arrest and Induction of Apoptosis

The effects of RGB-286147 on DNA replication, cell cycle progression, and tumor cell viability are described in Figure 2. Exposure of HCT116 cells to RGB-286147 (24/48 hr) caused a marked inhibition of DNA replication, as measured by a BrdU incorporation assay, and effects of >80% inhibition of DNA synthesis were observed at concentrations of RGB-286147 of 50–100 nM (Figure 2A). To determine the terminal phenotype associated with inhibition of DNA replication, a cell cycle analysis was performed with the same effective doses of RGB-286147 (Figure 2B). As shown, the majority of cells in an asynchronously dividing population of HCT116 cells were found in G1 and S phase, approximately 30% and 50%, respectively. Given that HCT116 cells divide with a doubling time of about 24 hr, reflecting cell cycle transit time, cell cycle effects of RGB-286147 were determined after 24 hr and 48 hr of incubation with RGB-286147. A pronounced accumulation of cells in G1 phase and a significant decrease in the

percentage of S phase cells were observed. Furthermore, an appearance of cells with >4N DNA content was observed at 24/48 hr with RGB-286147 at 100 nM. At both 24 and 48 hr, a significant accumulation of sub-G0/G1 cells had occurred, indicating the emergence of a population of apoptotic cells. Perhaps surprisingly, no accumulation of cells in G2/M phase was observed. In summary, the cell cycle studies show that RGB-286147 caused a pronounced G1 arrest, endoreduplication, and apoptotic cell death in HCT116 cells. Studies described below confirmed its marked effects on cell viability and its induction of apoptotic markers.

A fluorometric Calcein AM assay was used to quantitate effects of RGB-286147 on cell viability. Calcein AM is a substrate of intracellular esterases that are active only in viable cells. The cleavage of Calcein AM generates a fluorescent product that can be quantified on a fluorescence plate reader. The fluorescent signal is proportional to the number of viable cells. As shown in Figure 2C, RGB-286147 was a potent inhibitor of HCT116 cell viability. RGB-286147 was also found to affect the viability of asynchronously growing, nontransformed IMR90 human fibroblasts with similar potency. Clonogenic survival assays also revealed a potent and irreversible cell killing activity of RGB-286147 (Figure 2C). HCT116 cells were exposed to compound for 24 hr, then cultured for an additional 7 days in fresh media without compound. The fraction of cells that retained the ability to go through multiple rounds of cell division, and consequently form colonies, was then determined. The IC_{50} value for inhibition of colony formation by RGB-286147 was 57 nM. In conjunction with the cell cycle analysis, these findings suggest that a 24 hr exposure of HCT116 cells is sufficient to promote an irreversible, albeit delayed, cell death. RGB-286147 was more potent in this assay than flavopiridol. Exposure to RGB-286147 also induced an increase in annexin-V-positive cells (Figure 2D), a hallmark of apoptosis. Similarly, an increase in TUNEL-positive cells (as determined with a Terminal deoxynucleotidyl transferase dUTP Nick End Labeling assay) was observed upon exposure of HCT116 cells to RGB-286147 (data not shown). Exposure of HCT116 cells to RGB-286147 resulted in proteolytic cleavage of poly-ADP-ribose-polymerase (PARP), a known substrate for the caspase-3 apoptotic protease (Figure 2E); this finding is also consistent with an induction of apoptosis.

RGB-286147 Is a Broad-Spectrum Inhibitor of Tumor Cell Proliferation

The studies described above identified RGB-286147 as a potent inhibitor of cell cycle progression and the survival of HCT116 colon cancer cells. Here, we examined its activity profile across a broad panel of tumor cells of various genetic backgrounds and tissue origins. The Developmental Therapeutics program of the National Cancer Institute (NCI, US) provides a screening program through which compounds can be evaluated in a panel of 60 tumorigenic cell lines. This panel consists of cell lines expressing wild-type or mutant p53, p16-deficient and Rb mutant cell lines, and cell lines with various other genetic aberrations, including multidrug resistance. RGB-286147 was evaluated in this panel by the NCI and was found to be a highly potent and broad-spectrum inhibitor of tumor cell growth (Appendix S1; see the Supplemental Data available with this article online). The average GI_{50} for RGB-286147 at 48 hr of exposure was less than 10 nM. Interestingly, the GI_{50} value for the adriamycin/multidrug-resistant cell line NCI/ADR-RES was also less than 10 nM (with a TGI of 32–70 nM). Furthermore, the GI_{50} for the Rb-deficient prostate cancer cell line DU-145 was also less than 10 nM. Collectively, these results indicate that RGB-286147 is not subject to P-glycoprotein-mediated drug efflux, and that it is active against tumor cells with a variety of genetic aberrations, including Rb-deficient cells.

RGB-286147 Induces Cell Death in Noncycling HCT116 Tumor Cells

The proliferation of nontransformed, diploid cells, such as IMR90 human fibroblasts, requires the presence of growth factors, the removal of which leads to a decrease in cellular CDK activity and consequent exit from the cell cycle. Thus, as expected, serum withdrawal led to cell cycle arrest of cultured IMR90 cells, as measured by the BrdU incorporation assay (Figure 3A). HCT116 tumor cells also underwent cell cycle arrest in response to serum withdrawal. Most importantly, these effects were reversible. This was determined by a SNARF-1 viability assay (Figure 3A), a trypan-blue exclusion assay (data not shown), as well as a clonogenic assay. In the clonogenic assay, cells were cultured in the absence of serum for 6 days, trypsinized, collected, and replated in complete media (+FCS). More than 80% of the plated cells were capable of colony formation, indicating that serum-starved HCT116 cells were indeed in a state of reversible cell cycle arrest (the typical plating efficiencies of nonstarved cells would be similar). These observations allowed for an assessment of the effects of RGB-286147 on the viability of cell cycle-arrested cells as opposed to proliferating cells.

As shown in Figure 3B, RGB-286147 was equally active against noncycling as proliferating HCT116 cells. Similar results were obtained with several other compounds of this class (data not shown), as well as with flavopiridol. In contrast to flavopiridol, however, RGB-286147 was significantly less active toward quiescent versus proliferating IMR90 fibroblasts (more than 1–2 orders of magnitude less potent. Such observations were also made with several other related compounds; data not shown.). Exposure of arrested HCT116 cells to RGB-286147 also inhibited their ability to form colonies subsequent to refeeding with serum-supplemented culture medium. HCT116 cells were serum starved for 6 days and then exposed to RGB-286147 for 4 or 24 hr. Colony formation was assessed after an additional 5 days of growth in complete media. We observed a time- and dose-dependent loss of colony formation ability following exposure to RGB-286147 (Figure 3C). The untreated, serum-starved cells formed colonies upon refeeding with the same efficiency as nonstarved control cells maintained in complete media. Taken together, these results indicate that RGB-286147 inhibits the viability of HCT116 cells in the absence of cell cycle progression.

Target Profile of RGB-286147: Y3H-Based Proteome and Kinome Scanning

The cell cycle effects of RGB-286147, as well as its effects on the survival of both cycling and noncycling

A

	FCS	%BrdU+	% Viable
HCT116	+	68	90
	-	6	99
IMR90	+	20	82
	-	5	90

B

		Viability IC50 [μM]	
	FCS	RGB-286147	Flavopiridol
HCT116	+	0.040	0.221
	-	0.051	0.054
IMR90	+	0.012	0.278
	-	> 1	0.294

C

RGB-286147 [μM]	% inhibition of colony formation	
	4h	24h
0.050	0	90
0.100	25	100

Figure 3. RGB-186147 Promotes Tumor Cell Death in the Absence of Cell Cycle Progression

(A) Serum starvation (−FCS) causes inhibition of DNA replication in HCT116 cells and IMR90 fibroblasts, as determined by BrdU incorporation. Arrested cells remain viable, as determined by a SNARF-1 assay.

(B) RGB-286147 promotes cell death in proliferating (+FCS) and noncycling (−FCS) HCT116 cells (72 hr exposure). In contrast, RGB-286147 promotes cell death in proliferating, but not arrested, IMR90 cells. Effects of flavopiridol are also shown. Effects on viability of cells were determined by the Calcein AM assay. Calculated IC_{50} values for loss of viability in response to the various treatments are shown.

(C) Percent inhibition of colony formation by serum-starved HCT116 cells treated with RGB-286147. Cells were plated and serum starved for 6 days, exposed to the compound for the indicated period, and refed with complete media. Colony number was normalized to that obtained with untreated control cells also refed with complete media.

HCT116 cells, suggest that it may act on targets other than (or in addition to) CDK1 and CDK2. The following points support this supposition. First, it has been shown that CDK2 is not required for proliferation of various colon cancer cells, including HCT116 cells [11], and we have similarly found that CDK2-siRNA-induced downregulation of CDK2 does not inhibit proliferation of these cells (data not shown). However, we did find that RGB-286147 caused a pronounced G1 arrest (Figure 2B). Second, RGB-286147 induced endoreduplication, as indicated by the emergence of cells with >4N DNA content (see Figure 2B). Endoreduplicators are prone to undergo apoptotic cell death, and this could explain the emergence of the sub-G0/G1 cell population. It has been reported that inhibition of CDK1 renders fission yeast cells prone to chromosomal reduplication [39]. So, in principle, inhibition of CDK1 could have similar effects in mammalian cells. However, no accumulation of cells in G2/M was observed with RGB-286147, raising the question: is CDK1 actually inhibited by RGB-286147 (at 50–100 nM) to a significant extent in intact cells? It is also noteworthy that compounds that were less active than RGB-286147 toward CDK1 in vitro, such as RGB-285960 (IC_{50}: 310 nM), were as potent as RGB-286147 in inhibiting HCT116 proliferation (see Figure 1) and viability (IC_{50} for RGB-285960: 15 nM). These observations raise further doubt regarding the extent to which inhibition of CDK1 might have been implicated in the cytotoxic effects of RGB-286147.

Based on these considerations, we initiated a search for alternative targets of RGB-286147 by using the Y3H-based screening approaches we recently described [21]. The basic concept of the Y3H assay used in this study is briefly described in Figure 4A. As described previously, methotrexate-based hybrid ligands (methotrexate fusion compounds, MFCs) were used. SAR information that was available to us (e.g., as described in Figure 1), as well as the structural model highlighted in Figure 1C, suggested that positioning a polyethyleneglycol (PEG) spacer at the para position of the 6-benzyl substituent of RGB-286147 would not interfere with its inhibition of CDKs (and possibly other candidate kinases). As predicted, RGB-286276, a PEGylated analog of RGB-286147, retained CDK1- and CDK2-inhibitory activity as well as cellular activity (Figure 4B). Thus, two MFC derivatives of RGB-286147, RGB-286580 and a trichloro derivative, RGB-286156 (Figure 4C), were synthesized according to this strategy, which was described previously [21]. Both MFCs were assayed for yeast cell uptake and binding to DHFR by using an MFC competition assay (Figure 4D, see also Experimental Procedures for details). As shown, both test MFCs, RGB-286580 and RGB-286156, were found to permeate the yeast cells and bind to DHFR. Therefore, they provided suitable "baits" for screening and identification of target proteins. Two Y3H screening strategies were pursued: (1) random screening of human AD-cDNA libraries [21], which could lead to the identification of diverse target proteins (i.e., kinase and non-kinase targets); and (2) direct screening of robotically generated replica arrays of transformed yeast cells expressing individually cloned kinases/kinase domains (each array coordinate representing one specific kinase), many of which were previously found to interact with one or another small-molecule kinase inhibitor (approximately 250 such "functional" kinases, including S/T- and Y-kinases; data not shown). A total of approximately 500 cloned human kinases were represented in these yeast arrays (details of this clone collection will be published elsewhere). RGB-286512, a "universal" control that consists of MTX linked to the PEG spacer (MTX-PEG), and MTX-DEX, which consists of MTX linked to dexamethasone (DEX), were used as control compounds.

Figure 5A summarizes the Y3H screening results. For comparison, results obtained with RGB-286076, a purvalanol B-MFC we described earlier [21], were included. Several targets were identified, all of which encoded kinases. These included CDK1 (the weak signal is presumably due to the very weak expression of CDK1 in yeast; data not shown), CDK2, CDK3, CDK4, CDK5, and CDK6. Additional CDKs/CRKs included: CDK9, p42/CCRK (a CDK2-CAK), PCTK1 and PCTK3 (possibly PCTK2, although a comparably weak signal was

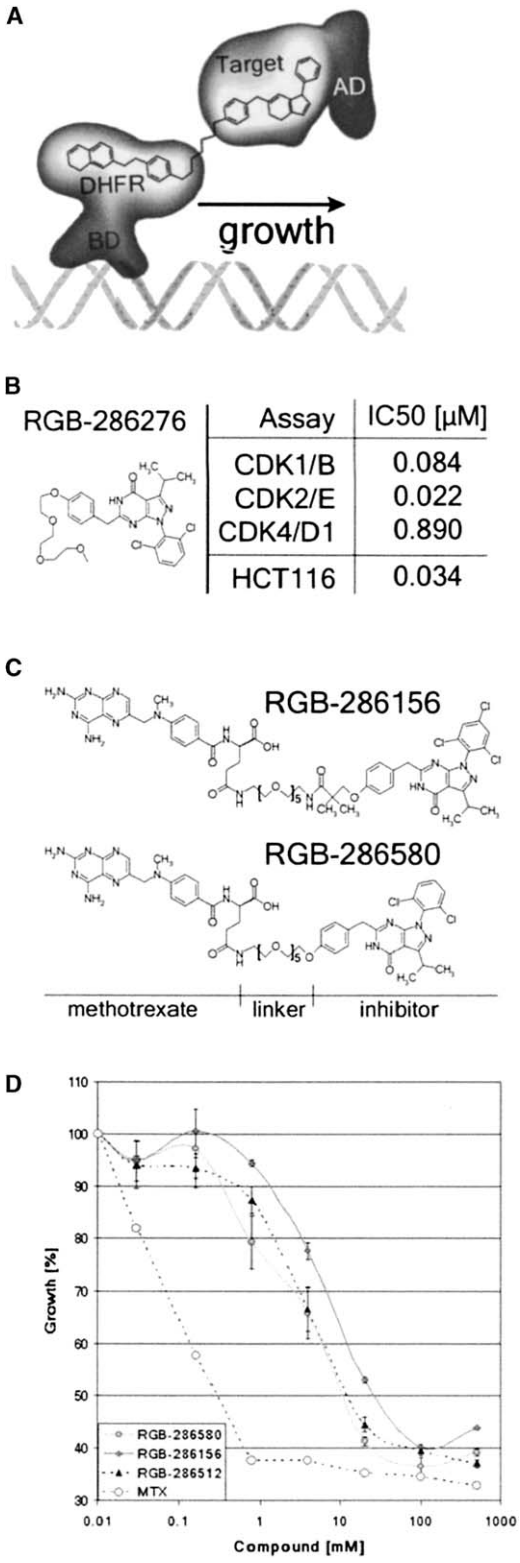

Figure 4. Y3H System and Chemical Dimerizers

(A) Schematic representation of the Y3H system.

(B) A PEGylated derivative of RGB-286147 (RGB-286276) retains CDK-inhibitory activity and inhibits HCT116 cell proliferation and viability (Calcein AM assay).

(C) Chemical structures of methotrexate-based chemical dimerizers (methotrexate fusion compounds, MFCs).

(D) Methotrexate and MFCs permeate yeast cells and prevent binding of a test peptide-AD fusion protein to DHFR. This 16-mer peptide was identified on the basis of its ability to bind DHFR in a methotrexate-sensitive fashion, providing an assay system for MFC competition experiments, as shown. Inhibition of the peptide-DHFR interaction, and consequently inhibition of HIS3 reporter activation, is reflected in a decrease in growth of yeast cells in the absence of histidine in the culture medium. Inhibition of growth in response to increasing concentrations of test MFCs is shown (error bars indicate standard deviations from the mean, n = 3 independent experiments).

detected, in particular, when compared to that observed for other kinase inhibitors; see [21]), and PFTK1. GSK3A represents a non-CRK kinase. Representative examples of "no hits," such as CSNK1D, E, LCK, FYN, and YES1, are also shown in Figure 5A; these, in contrast, scored positively with the purvalanol B-MFC (we have previously shown that purvalanol B also inhibits the enzyme activity of these kinases in vitro [21]). Similarly, RGB-286580 and RGB-286156 did not interact with several hundreds of other kinases that were part of the kinase array (data not shown). In contrast, the MFC incorporating purvalanol B, a purine analog and known CDK inhibitor, scored positively with a broad range of kinases other than CDKs (see also reference [21]), only a subset of which are shown in Figure 5A. A broad target spectrum was recently also described for yet another type of potent CDK inhibitor belonging to the chemical class of indenopyrazoles [21]. Thus, in comparison, the compounds described here display a remarkable specificity for CDK/CRK kinases in Y3H.

In order to validate the interactions identified with Y3H, in vitro small molecule-protein binding assays were performed. A PEGylated affinity chromatography probe, RGB-286051, was directly coupled to solid phase, as previously described [21]. Bead-immobilized compound was then incubated with cell extracts to determine its ability to bind to either endogenous or myc-tagged versions of the candidate targets. Bound proteins were eluted and subjected to immunoblot analysis (Figure 5B). For the detection of the binding of endogenous proteins to compound, cellular extracts derived from Jurkat, HCT116, or HEK293 cells were used. Extracts derived from transiently transfected HEK293 cells were used to detect binding of myc-tagged kinases/kinase domains by using an anti-myc tag antibody in the immunoblot analysis. As shown, specific binding to immobilized RGB-296051 was detected for endogenous CDK1, -2, -5, -7, and CDK9. Curiously, no binding for myc-tagged CDK9 was observed, the reason for which remains unclear. In addition, specific binding was observed for the myc-tagged forms of p42/CCRK, PCTK1, and PCTK3. In summary, the results described in Figure 5 suggest that RGB-286147 and related pyrazolopyrimidones exhibit a preferential affinity across the proteome for a relatively small group of CDK/CRK kinases.

Selectivity Profiling of RGB-286147: In Vitro Kinase Assays

RGB-286147 was profiled for activity against a panel of 69 recombinant kinases (Upstate) to further examine its selectivity profile (Figure 6A). Inhibitory effects on in

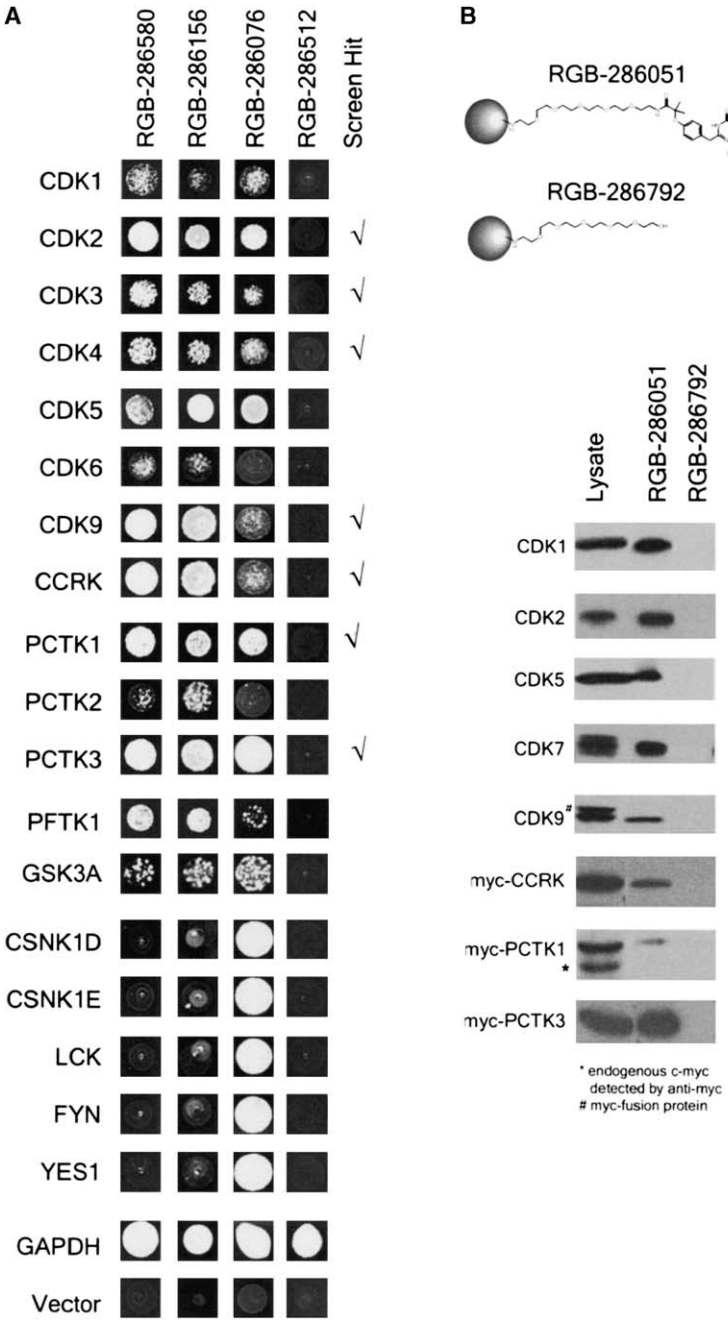

Figure 5. Identification of Novel Targets: Y3H Proteome Screening

(A) Y3H pyrazolopyrimidone MFC-target interactions. Interactions were originally identified via cDNA library screening (indicated by "screen hit" annotation) or direct screening of arrays of yeast cells transformed with individually cloned kinases. cDNA clones identified by the cDNA library screening approach were also used to retransform yeast cells and were subjected to array-based screening, as shown. A positive interaction is reflected in positive yeast cell growth (activation of HIS3 reporter). Arrays were interrogated with the indicated MFCs and a MTX-PEG "universal control." Images from each 96-well format array screen (one compound per array) were clustered to yield the composite image shown here.

(B) In vitro binding of endogenous proteins (Jurkat [CDK1, CDK2, CDK5], HCT116 [CDK7], or HEK293 cells [CDK9]) and exogenous, myc-tagged proteins (expressed in HEK293 cells) to a bead-immobilized pyrazolopyrimidone test compound, RGB-286051, or beads coupled to PEG spacer alone, RGB-286792. Protein binding was detected by immunoblot analysis with antibodies directed against endogenous proteins or the myc tag of the transgene-encoded fusion proteins, as indicated.

vitro kinase activity were first determined at a concentration of compound of 1 μM. As shown, 8 out of 69 kinases that were evaluated scored positive (≥50% inhibition). IC_{50} values were subsequently determined for these particular kinases (Figure 6B). In addition to potently inhibiting CDK1 and CDK2, RGB-286147 inhibited the kinase activity of CDK3, CDK5, and CDK7, with similar potency (low nanomolar IC_{50} values). Comparatively, RGB-286147 only weakly inhibited CDK4, CDK6, and GSK3b (higher nM–μM range IC_{50} values).

CDK9 IP-kinase assays confirmed that RGB-286147 is also a potent inhibitor of cellular CDK9 (Figure 6C). The effects of RGB-286147 were compared to those of flavopiridol, a reportedly potent CDK9 inhibitor [40, 41] (reported IC_{50} for CDK9 inhibition: 5–10 nM). Both compounds inhibited the autophosphorylation of CDK9 as well as the crossphosphorylation of cyclin T1 by CDK9 in a dose-dependent manner and with comparable potency. Similar effects were observed when assaying the phosphorylation of the C-terminal domain (CTD) of RNA pol II, a natural substrate for CDK9. The relative activity of RGB-286147 toward CCRK and the PCTKs remains to be determined. In summary, the results described in Figures 6 and 7 further suggest that RGB-286147 and related analogs exhibit a high degree of specificity for CDK/CRK kinases.

Inhibition of CDKs by RGB-286147 in Intact Cells

A common view is that phosphorylation of Rb is triggered by CDK4/6 kinases and probably completed by

A

Kinase	% inhibition at 1 μM of RGB-286147
CDK1/CycB; CDK2/CycA; CDK2/CycE; CDK3/CycE; CDK5/p35; CDK7/CycH/MAT1	> 90%
CDK6/CycD3; GSK3β	60 - 70%
CAMKII; CK1;JNK3	20-30%
CK2; cSRC; FYN; IKKα; IR; MKK6; PAK2; RSK1; RSK2; RSK3; SAPK2a; SAPK3;	10-20%
ABL; AMPK; BLK; CAMKIV; CHK1; CHK2; c-RAF; CSK; FES; FGFR3; IGF-1R; IKKβ; JNK1α1; JNK2α2; LCK; LYN; MAPK1; MAPK2; MAPKAP-K2; MEK1; MKK4; MKK6; MKK7β; MSK1; P70S6K; PDGFRα; PDGFRβ; PDK1; PKA; PKBα; PKBβ; PKCα; PKCβII; PKCγ; PKCθ; PKCε; PRAK; PRK2; SAPK2b; SAPK4; SGK; SYK; ROCK-II; YES; ZAP-70	< 10%

B

Kinase	RGB-286147 IC50 [μM]
CDK1/B	0.048
CDK2/E	0.015
CDK3/E	0.009
CDK4/D1	0.839
CDK5/p35	0.010
CDK6/D3	0.282
CDK7/H/MAT1	0.071
GSK3β	0.754

C

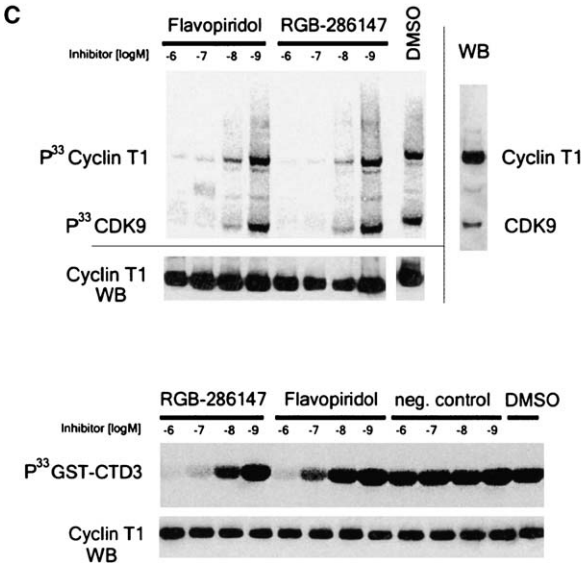

Figure 6. Selectivity Profiling of RGB-286147

(A) Inhibition of in vitro kinase activity of purified kinases by RGB-286147. Percent inhibition at 1 μM compound is shown.

(B) IC_{50} values for inhibition of kinase activity by RGB-286147.

(C) Inhibition of CDK9 kinase activity by RGB-286147. CDK9 IP-kinase assays were performed, as indicated, measuring either CDK9 autophosphorylation and cyclin T1 crossphosphorylation (upper panel) or phosphorylation of purified CTD3 (C-terminal domain of RNA ploymerase II, a natural substrate of CDK9, lower panel). The total amount of cyclin T1 in each immunoprecipitate was also determined by immunoblotting in order to control for the potential difference in sample loading. WB: Western blot analysis for cyclin T1 and/or CDK9, as indicated.

CDK2 as cells enter S phase. Here, we assessed the effects of RGB-286147 on the phosphorylation status of Rb, as well as other cell cycle regulatory proteins (Figure 7). As expected for a compound that promotes G1 arrest and a decrease in the number of cells in S phase, RGB-286147 caused a significant reduction in cyclin A expression. RGB-286147 also caused a reduction in phosphorylation of Rb on Ser807/811 (CDK2 phosphorylation sites) as well as Ser795 and Ser780 (CDK4 phosphorylation sites), suggesting that RGB-286147 inhibits the activity of CDK4/6, and perhaps that of CDK2, in cells. Recent observations made by Tetsu and McCormick [11] indicate that inhibition of CDK4/6, but not CDK2, reduces phosphorylation of Rb at Ser807/811 in HCT116 cells. They hypothesized that the unusually high level of CDK4/6 activity in these cells, due to loss of p16/INK4a, upregulation of cyclin D1 (through Ras and β-catenin), and expression of the assembly factor p21/Cip1, was sufficient to promote crossphosphorylation and make CDK2 redundant. Accordingly, the decrease in Ser807/811 phosphorylation caused by RGB-286147 was more likely due to inhibition of CDK4/6. CDK4/6 was not strongly inhibited by RGB-286147 in vitro. However, RGB-286147 caused a marked reduction in cyclin D1 levels, an effect known to result in a decrease in CDK4 activity in HCT116 cells [11].

Analysis of the phosphorylation status of CDK2 showed that RGB-286147 also caused a significant decrease in the levels of the p-Thr160-phosphorylated form of CDK2. Phosphorylation of CDK2 at Thr160 is required for its activation [6]. CDK7 and CCRK [7], which have been shown to exhibit CDK2-activating activity, were both found to be targets for RGB-286147. Thus, inhibition of one or both of these kinases may contribute to the overall effects of RGB-286147 on CDK2 activation. CDK7 also exhibits CDK1/4-activating activity. It remains unclear, however, whether RGB-286147 also had an effect on activation of these kinases. Whether CDK4/6 is a substrate for CCRK is also unclear. In summary, RGB-286147 caused a significant inhibition of CDK2 and CDK4/6 activity in HCT116 cells. Inhibition of CDK4/6 in HCT116 cells is sufficient to cause G1 arrest and inhibition of proliferation of HCT116 cells [11, 42]. Thus, indirect inhibition of CDK4/6 provides one plausible mechanism for the G1 arrest induced by RGB-286147 in HCT116 cells.

Discussion

In the present study, we undertook a first step toward a more detailed analysis of the pharmacological properties and therapeutic potential of compounds that are

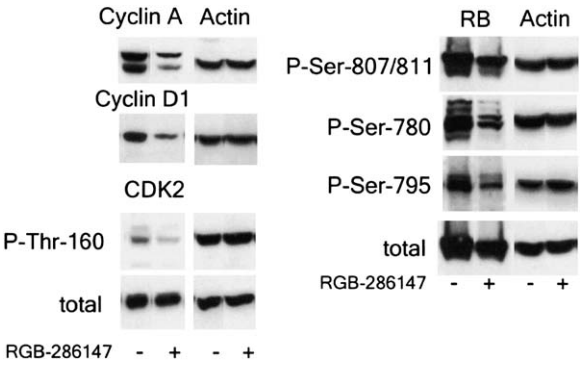

Figure 7. Effects of RGB-286147 on Cell Cycle Regulatory Proteins in Intact Cells

Effects of RGB-286147 on the expression levels of various cell cycle regulatory proteins (cyclin A, cyclin D1, CDK2) and phosphorylated forms of Rb and CDK2. HCT116 cells were incubated for 24 hr (100 nM RGB-286147) prior to analysis by immunoblotting with antibodies specific for the respective protein/phosphoproteins.

based on a [1, 3, 6]-tri-substituted-pyrazolo[3,4-d]-pyrimidine-4-one CDK kinase inhibitor scaffold. Compounds of this class were recently shown to inhibit the in vitro kinase activity of CDK1 and CDK2 [38], but the molecular basis for their antiproliferative and antitumor activities remained unclear. Our analysis of related analogs, such as RGB-286147, indicates that compounds of this chemical class can exhibit a more complex range of antitumor activities than previously recognized, and that these activities involve targets in addition to or other than CDK1 and CDK2. The cell killing activity of RGB-286147 in noncycling HCT116 colon cancer cells, but not in quiescent nontransformed fibroblasts, is particularly intriguing and suggests that exploring the MoA of this compound and related analogs could yield new insights into mechanisms regulating the survival of tumor cells that are not actively engaged in cell cycle progression.

The HCT116-antiproliferative activities of RGB-286147 are reflected in a pronounced decrease in the number of S phase cells and a concomitant accumulation of cells in G1 phase of the cell cycle. Although RGB-286147 appears to inhibit CDK2 in HCT116 colon cancer cells, the G1 cell cycle-inhibitory effect appears to be mediated through an inhibition of CDK4. RGB-286147 is not a potent inhibitor of purified CDK4/cyclin D1 (or CDK6/cyclin D3). However, in cells, RGB-286147 caused a decrease in the expression of cyclin D1, one of its regulatory components, an effect known to result in a decrease in CDK4 activity in HCT116 cells [11]. Whether CDK4/6 could also be inhibited by other mechanisms remains to be explored. Inhibition of CDK7 by RGB-286147 could possibly interfere with the activation of CDK4/6 [6]. Another interesting possibility may involve the CDK-activating kinase p42/CCRK. This kinase has recently been reported to act as a CDK2 (but not CDK1)-activating kinase [7]. CDK2 activation appears to be inhibited by RGB-286147, which could have involved inhibition of p42/CCRK. Furthermore, interference with p42/CCRK activity or expression has recently been reported to cause a G1 cell cycle arrest in HeLa cells [7], which, similar to HCT116 colon cancer cells, do not appear to require CDK2 for cell cycle progression [11]. Therefore, it is conceivable that RGB-286147 induces G1 arrest in HCT116 cells through inhibition of p42/CCRK and substrates other than CDK2. A further clarification of the effects of RGB-286147, and related analogs, on p42/CCRK in cells may facilitate the functional characterization of this interesting kinase.

Besides perturbing cell cycle progression, we also found RGB-286147 to induce a pronounced apoptotic cell death in HCT116 colon cancer cells. RGB-286147 was also active against cell cycle-arrested HCT116 cells. In contrast, RGB-286147 inhibited the proliferation and viability of nontransformed human fibroblasts (IMR90 cells), but was inactive toward these cells when in the quiescent state. Only a limited number of cancer cells in established tumors do cycle at any point in time, which poses a problem for many chemotherapeutic drugs that are primarily active against cycling tumor cells. Gaining insights into mechanisms that regulate the survival of noncycling tumor cells could lead to new drug discovery strategies. RGB-286147 provides a promising molecular probe for such investigations. Inhibition of CDK1, CDK2, or CDK4 is not likely to play a major role in the cytotoxic effects of RGB-286147 in serum-starved/non-cycling HCT116 cells, as it is presumed that, in these cells, these kinases are in an inactive state. This supposition is also supported by the recent findings that highly selective small-molecule inhibitors of CDK4/6 induce a reversible G1 arrest in the Rb-positive HCT116 cells while having no effect on Rb-negative tumor cells [11, 42]. Furthermore, as already discussed, neither CDK2 nor CDK1 are likely to be the sole or primary mediators of the cytotoxic effects of RGB-286147 in cycling HCT116 cells. On the other hand, the proteome profiling efforts described here reveal a first set of candidate targets that could be investigated in this context. RGB-286147 targets that we identified include: CDK3, CDK5, CDK7, CDK9, p42/CCRK, PCTK1/3, and PFTK1. CDK3 has been reported to play a role in promoting G0 exit [43], and mice develop normally in the absence of functional CDK3 [44]. CDK5 has been linked primarily to neuronal and secretory cell functions [4, 15]. Thus, neither of these kinases is a likely mediator of the cytotoxic activites of RGB-286147, and future studies should arguably focus on the remaining kinases, the functions of some of which are currently only poorly understood.

The finding that RGB-286147 and its derivatives exhibit a highly specific and arguably narrow CDK/CRK target profile should facilitate the design and characterization of novel analogs with subtle differences in selectivity profiles. We have recently indeed identified analogs that exhibit significant differences in their CDK selectivity profiles (unpublished data). For example, compounds with higher selectivity for CDK5 or CDK9 could have therapeutic applications in indications other than cancer. CDK5 plays a role in neuronal and secretory cell functions and has emerged as an interesting candidate target for inhibition of neuronal cell death. CDK9 has recently been implicated in the pathogenesis of cardiac hypertrophic growth and as a permissive host factor in HIV-1 replication [17]. Roscovitine (or CYC202), a reported CDK1/2/5/7/9 inhibitor, has recently been

shown to repress cellular CDK9 kinase activity and HIV transcription, and to induce apoptosis in HIV-1-infected cells, an effect not observed in uninfected control cells [45]. This and other studies [17, 18] suggest that inhibition of CDK9 could be a strategy for the development of a novel generation of AIDS therapeutics. Thus, the observation that [1, 3, 6]-tri-substituted-pyrazolo[3,4-d]-pyrimidine-4-one analogs exhibit potent CDK5- and CDK9 kinase-inhibitory activities, while targeting a narrow spectrum of CDKs/CRKs (compared to other CDK inhibitor chemotypes [21]), suggests that this chemical class should be further examined for the design of novel, potentially even more selective kinase inhibitors with applications to therapeutic areas other than cancer. Finally, this study further highlights the utility of Y3H screening in drug MoA studies. We anticipate that Y3H screening will prove to be generally useful in the identification of targets for various kinase inhibitor chemotypes, as well as other classes of organic small molecules.

Significance

The realization that small-molecule inhibitors of protein kinases might be of therapeutic use, as exemplified by the use of phenylaminopyrimidine STI571 (also known as imatinib mesylate or Gleevec) in the treatment of chronic myelogenous leukemia, has led to intensive drug discovery efforts around multiple disease-relevant kinases. These include the subfamily of cyclin-dependent kinases (CDKs) and CDK-related (CRK) kinases. Due to the potential of ATP-competitive kinase inhibitors to crossreact with multiple, even phylogenetically distantly related, kinases, identifying their targets is a critical challenge in validating their use as potential therapeutic agents or as molecular probes. Here, we used a chemical proteomics approach to explore the mechanisms of action and potential applications of compounds derived from a [1, 3, 6]-tri-substituted-pyrazolo[3,4-d]-pyrimidine-4-one kinase inhibitor scaffold. Our results suggest that this class of compounds exhibits a remarkable specificity for kinases of the CDK/CRK subfamily of protein kinases, and a source of novel molecular probes for exploring mechanisms that regulate tumor cell survival in the presence and/or absence of cell cycle progression. Our results also suggest that the [1, 3, 6]-tri-substituted-pyrazolo[3,4-d]-pyrimidine-4-one scaffold may be further exploited for the design of proteome-wide CDK/CRK-specific kinase inhibitors with various therapeutic applications. Finally, this study further highlights the potential for Y3H in the identification of novel kinase inhibitor targets. Y3H should be equally applicable to the study of other types of organic small molecules.

Experimental Procedures

Compound Synthesis

Details of an example MFC synthesis (RGB-286580) are provided in the Supplemental Data (Appendix S2). The other [1, 3, 6]-tri-substituted-pyrazolo[3,4-d]-pyrimidine-4-one analogs were synthesized by procedures similar to the synthesis of Compound 1 in Appendix S2.

Molecular Modeling

Using program FlexX [46], the inhibitor RGB-286147 was docked into the ATP binding site of CDK2 (PDB entry 1ckp). A 6.5 Å distance cut-off for the ATP binding site was applied; water and inhibitor molecules were excluded from the calculation. The model that was obtained is in agreement with the recently published X-ray structure of CDK2 in complex with a comparable pyrazolo-pyrimidin-4-one compound [38]. The picture was rendered with ViewerPro (Accelsys) and Povray (http://www.povray.org).

In Vitro Kinase Assays

CDK kinases and cyclins were expressed in Sf9 insect cells. CDK/cyclin complexes were purified and assayed as described previously [47]. Alternatively, the effects of compounds on kinase activity were tested at Upstate Biotechnology.

Cell Culture and Viability Assays

HCT116 colon carcinoma cells (ATCC) were grown in RPMI-1640 supplemented with 10% FCS in a humidified incubator at 37ºC and 5% CO_2. Viability was measured in a 24-well format (1,000 cells per well) with the Calcein AM assay (Molecular Probes). The fluorescent, viable cells were quantitated with a Cytofluor II fluorescent plate reader (PE Biosystems). The clonogenic survival of cells treated with RGB-286147 was determined by treating 10,000 cells grown in 15 cm plates with the compound for 24 hr, followed by a 7 day outgrowth in media without compound. Colony number was determined by manual counting of cells stained with 0.4% crystal violet in 20% ethanol. Cellular proliferation was determined with the Sulforhodamine B (SRB) assay [48]. HCT116 cells were grown in 96-well microtiter plates (1,000 cells/well) and were exposed to the compounds for 72 hr. The cells were fixed with cold TCA to a final concentration of 10% and incubated at 4ºC for 60 min. The plates were then washed five times with water and air dried. SRB solution at 0.4% (w/v) in 1% acetic acid was added to each well, and the plates were incubated for 10 min at room temperature. The plates were washed five times with 1% acetic acid and air dried. The bound stain was then solubilized with 10 mM trizma base, and the absorbance was read on a plate reader at 570 nM.

Cell Cycle Analysis

HCT116 cells were harvested from subconfluent plates, and 100,000 cells were treated with a range of doses of RGB-286147 for 24 or 48 hr. At the indicated time, the adherent cells were recovered by trypsinization, combined with the floaters, and collected by centrifugation. Medium was decanted from the cell pellet, and 100 μl PI stain-1, which contains 50 μg/ml propidium iodide, 3% PEG 6000, 180 U/ml RNase, 0.1% Triton-X, 3.6 mM citrate buffer (pH 7.2), was added to the cell pellet. The cells were incubated at 37ºC for 20 min, after which 100 μl PI stain-2, which contains 3% PEG 6000, 50 μg/ml propidium iodide, 0.1% Triton-X, and 0.375 M NaCl (pH 7.2), was added to the cells. The cells were incubated at 4ºC for 1 hr and analyzed on a Becton Dickenson FACScan flow cytometer fitted with ModFit LT cell cycle analysis software (Verity Software House, Inc.). The effect of RGB-286147 on DNA replication was measured with BrdU in a flow cytometric assay. HCT116 cells (100,000 cells /T-25 flask) were cultured in the presence of RGB-286147 for a period of 24 or 48 hr before the addition of BrdU (10 μM final concentration), after which the incubation was continued for 16–18 hr. Incorporation of BrdU was determined with the BrdU Flow Kit (BD-Pharmingen) according to the manufacturer's specifications and was quantified on the flow cytometer.

Analysis of Apoptosis

HCT116 cells (1×10^5 per T75 flask) were treated with 50 nM RGB-286147 for 48 hr. The cells were recovered by trypsinization, were incubated with a buffer containing AnnexinV-FITC and propidium iodide according to the manufacturer's specification (BD Pharmingen #556547), and were analyzed by flow cytometry.

Arrested Cell Assay

The cytotoxicity of RGB-286147 was determined on arrested normal fibroblasts, IMR90, and tumorigenic cells, HCT116. IMR90 cells were plated in triplicate for each compound concentration to be tested in MEM-α media containing 10% fetal calf serum at a density

of either 2,000 or 20,000 cells per well in 24-well dishes and were incubated overnight at 37ºC, 5% CO_2. The media was replaced from the 20,000 cells per well dish with serum-free media after washing once with the same, while the wells containing 2,000 cells were maintained in complete media. The plates were incubated for 3 additional days. HCT116 cells were plated in triplicate for each compound concentration to be tested in RPMI 1640 media containing 10% fetal calf serum at a density of either 200 or 2,000 cells per well in 24-well dishes and were incubated overnight at 37ºC, 5% CO_2. The media from the 2,000 cells per well dish were replaced with serum-free media after washing once with the same. It had been established in a prior experiment that the HCT116 cells required 6 days to arrest in response to serum starvation, so the plates were incubated for this period of time. The cells were exposed to a dose range of RGB-286147 for 72 hr in the absence of serum, and the effect on viability was determined with the Calcein AM assay as described above. In order to ensure that the cells had indeed exited the cell cycle upon serum withdrawal, the percentage of BrdU-positive cells was determined in each experiment. In these experiments, cellular viability and cell cycle progression were evaluated simultaneously by flow cytometry. For this purpose, cell viability was determined with the use of SNARF-1, a red fluorescent alternative to Calcein. With this method, cells can be costained with FITC (green fluorescence) to detect BrdU and SNARF-1 (red fluorescence) to measure viability. Together, the evaluation of BrdU incorporation and SNARF-1 cleavage by flow cytometry provides an assessment of the viability of arrested cells. The cells were stained with SNARF-1 as follows and then prepared for determination of BrdU incorporation as described above. A 5 μg/ml solution of SNARF-1 (Molecular Probes) was prepared by dissolving 50 μg SNARF-1 in 50 μl DMSO and dilution into 10 ml PBS. This stock was further diluted 1:64,000, and 200 μl was added to each tube of cells that had been previously pulsed with BrdU. The cells were incubated at 37ºC for 30 min and washed with 3 ml PBS. The cells were then fixed and prepared for the measurement of BrdU as described above.

Bacterial and Yeast Strains

E. coli strain DH10B (Life Technologies) was used for all bacterial work in this study. The *Saccharomyces cerevisiae* strain used in this study was strain 6A (GPC Biotech AG; *MATa*, *his3-Δ200, trp1-901, leu2-3,112, LYS2*::[*4lexAop*HIS3], *ade2*::[*6lexAopURA3*], *ura3*::[*8lexAopLacZ*], *GAL4*, *gal80, can1, cyh2*). The strain enables the use of a LexA binding domain-based protein interaction systems using the HIS3 and/or LacZ reporters and the use of cDNA libraries fused to the GAL4p activation domain (AD). Yeast cells were grown in synthetic dextrose (SD) media with appropriate auxotrophic supplements [49]. Standard genetic methods were followed.

Plasmids

Plasmid pBYK-DHFR was described before [21]. A variant of pACT2 (Clontech), which was compatible for use with the GATEWAY in vitro recombination cloning system (Invitrogen), was generated and used for directional cloning of cDNAs encoding specific kinases.

Competition Experiments

We previously identified a 16-mer peptide (RLGSPSGVLDMYCRLH)-AD fusion that interacts with DHFR. Binding of methotrexate to DHFR prevents this interaction. Similarly, binding of an MFC to DHFR interferes with this interaction. Thus, the successful uptake of an MFC into yeast and its binding to DHFR can be measured as a function of a decrease in HIS3 reporter activity (reflected in dose-dependent inhibition of cell growth) induced by expression of the peptide-AD fusion protein and LexA-DHFR. To test for growth competition, either 1 μl DMSO (negative control, 100% growth) or 1 μl test MFC at an appropriate concentration was added. Yeast cell growth was monitored and quantified by measuring the optical density of the culture at day three at a wavelength of 600 nm.

cDNA Libraries

Strain 6A + pBYK-DHFR was transformed by using the lithium acetate method [37]. pACT2-based cDNA libraries were purchased from Clontech: human brain, liver, heart, and placenta. All libraries encoded polypeptides fused to the carboxy terminus of the GAL4 activation domain. The total number of independent yeast colonies reflected at least 1× the complexity of independent clones documented for the *E. coli* library, as specified by the manufacturer. The yeast libraries were harvested, quality control tested, and stored in small aliquots at −70ºC.

cDNA Library Screening and Array Screening

The screening of cDNA libraries and kinase arrays with RGB-286580 and RGB-286156 was performed as described previously [21]. RGB-286580 exhibited some autoactivating activity. This could be easily suppressed by the addition of 10 mM 3-amino-1,2,4-triazole.

Binding of RGB-286051 to Kinase Targets In Vitro

A PEGylated pyrazolopyrimidone CDK inhibitor (RGB-286051) or a 5 PEG-amine linker (RGB-286792) was coupled to ReactiGel agarose beads (Pierce, No. 20259) as previously described [28]. Pull-downs were essentially performed as previously described [28]. In vitro binding of endogenous proteins was detected by using extracts of Jurkat (CDK1, CDK2, CDK5), HCT116 (CDK7), or HEK293 cells (CDK9). Exogenous myc-tagged proteins were expressed in HEK293 cells. Protein binding was detected by immunoblot analysis with antibodies directed against endogenous proteins or the myc tag of transgene-encoded fusion proteins, as indicated. Immobilized PEG spacer (RGB-286792) served as control.

CDK9 IP-Kinase Assays

Subconfluent plates of PC-3 cells (ATCC) were lysed in 4 ml RIPA buffer (20 mM Tris-HCl [pH 8.0], 0.5% Nonidet P-40, 1% Triton X-100, 150 mM KCl, 5 mM dithiothreitol) containing protease and phophatase inhibitors (Roche). Lysates were clarified by centrifugation and subsequently precleared by 30 min of incubation with Protein A sepharose (CL4B) beads. Lysates were then incubated with mouse anti-human CDK9 monoclonal antibody for 2 hr at 4ºC. The antigen-antibody complex was precipitated by incubation with Protein A sepharose (CL4B) beads (Amersham Bioscience Corp. 17-0780-01) for 1 hr at 4ºC. The beads were pelleted and washed 5 times in 1 M KCl wash buffer (20 mM Tris-HCl [pH 8.0], 0.5% Nonidet P-40, 1% Triton X-100, 1 M KCl), once in assay buffer, then resuspended in assay buffer (20 mM Tris-HCl [pH 8.0], 5 mM $MgCl_2$, 60 mM NaCl) and aliquoted into 96-well plates. Compounds were dissolved in DMSO, diluted into assay buffer lacking ATP (final DMSO is less then 0.1%), and preincubated for 20 min with CDK9 captured on sepharose beads. CDK9 autophosphorylation, cyclin T1 crossphosphorylation, or GST-CTD3 (~2 μg per sample) phosphorylation reactions were started by addition of ATP to the reaction mixtures (final concentration: 10 μM ATP and 10 μCi ^{33}P-ATP). The phosphorylation reactions were stopped after 15 min at 37ºC by addition of SDS-PAGE loading buffer and heating of the sample to 96ºC. The samples were then analyzed by 4%–12% SDS-PAGE followed by blotting onto nitrocellulose (BIO-RAD Laboratories, 162-0233) membrane. Phosphorylation was detected on a Fuji Bas-5000 β-imager.

For detection of CDK9 and cyclin T1 by immunoblotting, the membrane was incubated with mouse anti-human CDK9 or goat anti-human cyclin T1 (SC-8127 Santa Cruz Biotechnology, Inc.), followed by incubation with anti-mouse or goat HRP-conjugated secondary antibody. Signals were detected by using ECL (Amersham Biosciences Corp.) and autoradiography.

Effects of RGB-286147 on Cell Cycle Proteins in Intact Cells

HCT116 cells were treated with RGB-286147 (100 nM) for 24 hr. Cells (adherent as well as floating cells) were collected. Lysis was performed following a protocol adapted from Romero et al. [50], and cell extracts were stored at −80ºC. Immunoblot analysis of cell lysates was performed by using antibodies as indicated. Immunoblots were blotted with an anti-actin antibody as a loading control. Antibodies that were used were specific for: CDK2 (32 kDa), P-Thr160-CDK2 (32 kDa), cyclin A (60 kDa), Rb (110 kDa), P-Ser780-Rb, P-Ser795-Rb, and P-Ser807/811-Rb. The effect on PARP cleavage was analyzed as follows: HCT116 cells were treated with 100 nM RGB-286147 for 48 hr and compared to untreated cells. PARP (116 kDa) and its cleaved form (89 kDa) were detected by using a PARP-specific antibody.

Antibodies

The following primary antibodies were used in this study: anti-actin (I-19), anti-CDK5 (DC 17), anti-CDK9 (D-7), anti-CDK1 (17), and anti-CDK7 (C-14) were from Santa Cruz; anti-P-CDK2 (Thr160), anti-cyclin D1 (DCS6), anti-PARP, anti-P-Rb (Ser780), anti-P-Rb (Ser795), anti-P-Rb (Ser807/811), and anti-Rb (4H1) were from Cell Signaling; anti-cyclin A (25) and anti-CDK2 (55) were from BD Transduction Laboratories; and anti-c-*myc* (9E10) was from Roche. The secondary antibodies were from Zytomed (goat anti-rabbit IgG-HRP and rabbit anti-goat IgG-HRP), Sigma (goat anti-mouse IgG-HRP), and Amersham (sheep anti-mouse IgG-HRP).

Supplemental Data

Supplemental Data including details on MFC chemical synthesis and antiproliferative effects of RGB-286147 in various human tumor cell lines are available at http://www.chembiol.com/cgi/content/full/12/10/1103/DC1/.

Acknowledgments

We thank Dr. Margaret Lee Kley for critical reading of the manuscript and helpful comments. We also thank Dr. Robert Schultz (National Cancer Institute [NCI], Bethesda, MD) for screening RGB-286147 in the NCI 60 tumor cell line panel; D. Karafilidis, P. Sebastian, C. Degenhart, and S. Dill for technical assistance; and J. Vogt for molecular modeling. This work was supported in part by the German Ministry for Education and Research (Bundesministerium fuer Bildung und Forschung [BMBF], Biochance Grant Nr. 0312451 to GPC Biotech AG, N.K.).

Received: June 17, 2005
Revised: August 5, 2005
Accepted: August 8, 2005
Published: October 21, 2005

References

1. Morgan, D.O. (1997). Cyclin-dependent kinases: engines, clocks, and microprocessors. Annu. Rev. Cell Dev. Biol. *13*, 261–291.
2. Sherr, C.J., and McCormick, F. (2002). The RB and p53 pathways in cancer. Cancer Cell *2*, 103–112.
3. Knockaert, M., Greengard, P., and Meijer, L. (2002). Pharmacological inhibitors of cyclin-dependent kinases. Trends Pharmacol. Sci. *23*, 417–425.
4. Fischer, P.M., Endicott, J., and Meijer, L. (2003). Cyclin-dependent kinase inhibitors. Prog. Cell Cycle Res. *5*, 235–248.
5. Lyon, M.A., Ducruet, A.P., Wipf, P., and Lazo, J.S. (2002). Dual-specificity phosphatases as targets for antineoplastic agents. Nat. Rev. Drug Discov. *1*, 961–976.
6. Kaldis, P. (1999). The cdk-activating kinase (CAK): from yeast to mammals. Cell. Mol. Life Sci. *55*, 284–296.
7. Liu, Y., Wu, C., and Galaktionov, K. (2004). p42, a novel cyclin-dependent kinase-activating kinase in mammalian cells. J. Biol. Chem. *279*, 4507–4514.
8. Fattaey, A., and Booher, R.N. (1997). Myt1: a Wee1-type kinase that phosphorylates Cdc2 on residue Thr14. Prog. Cell Cycle Res. *3*, 233–240.
9. Sherr, C.J., and Roberts, J.M. (2004). Living with or without cyclins and cyclin-dependent kinases. Genes Dev. *18*, 2699–2711.
10. Ortega, S., Prieto, I., Odajima, J., Martin, A., Dubus, P., Sotillo, R., Barbero, J.L., Malumbres, M., and Barbacid, M. (2003). Cyclin-dependent kinase 2 is essential for meiosis but not for mitotic cell division in mice. Nat. Genet. *35*, 25–31.
11. Tetsu, O., and McCormick, F. (2003). Proliferation of cancer cells despite CDK2 inhibition. Cancer Cell *3*, 233–245.
12. Chen, Y.N., Sharma, S.K., Ramsey, T.M., Jiang, L., Martin, M.S., Baker, K., Adams, P.D., Bair, K.W., and Kaelin, W.G., Jr. (1999). Selective killing of transformed cells by cyclin/cyclin-dependent kinase 2 antagonists. Proc. Natl. Acad. Sci. USA *96*, 4325–4329.
13. Lees, J.A., and Weinberg, R.A. (1999). Tossing monkey wrenches into the clock: new ways of treating cancer. Proc. Natl. Acad. Sci. USA *96*, 4221–4223.
14. Du, J., Widlund, H.R., Horstmann, M.A., Ramaswamy, S., Ross, K., Huber, W.E., Nishimura, E.K., Golub, T.R., and Fisher, D.E. (2004). Critical role of CDK2 for melanoma growth linked to its melanocyte-specific transcriptional regulation by MITF. Cancer Cell *6*, 565–576.
15. Borgne, A., and Golsteyn, R.M. (2003). The role of cyclin-dependent kinases in apoptosis. Prog. Cell Cycle Res. *5*, 453–459.
16. Monaco, E.A., 3rd, and Vallano, M.L. (2003). Cyclin-dependent kinase inhibitors: cancer killers to neuronal guardians. Curr. Med. Chem. *10*, 367–379.
17. De Falco, G., and Giordano, A. (2002). CDK9: from basal transcription to cancer and AIDS. Cancer Biol. Ther. *1*, 342–347.
18. Chiu, Y.L., Cao, H., Jacque, J.M., Stevenson, M., and Rana, T.M. (2004). Inhibition of human immunodeficiency virus type 1 replication by RNA interference directed against human transcription elongation factor P-TEFb (CDK9/CyclinT1). J. Virol. *78*, 2517–2529.
19. Sano, M., Abdellatif, M., Oh, H., Xie, M., Bagella, L., Giordano, A., Michael, L.H., DeMayo, F.J., and Schneider, M.D. (2002). Activation and function of cyclin T-Cdk9 (positive transcription elongation factor-b) in cardiac muscle-cell hypertrophy. Nat. Med. *8*, 1310–1317.
20. Sano, M., and Schneider, M.D. (2003). Cyclins that don't cycle–cyclin T/cyclin-dependent kinase-9 determines cardiac muscle cell size. Cell Cycle *2*, 99–104.
21. Becker, F., Murthi, K., Smith, C., Come, J., Costa-Roldan, N., Kaufmann, C., Hanke, U., Degenhart, C., Baumann, S., Wallner, W., et al. (2004). A three-hybrid approach to scanning the proteome for targets of small molecule kinase inhibitors. Chem. Biol. *11*, 211–223.
22. Daub, H., Godl, K., Brehmer, D., Klebl, B., and Muller, G. (2004). Evaluation of kinase inhibitor selectivity by chemical proteomics. Assay Drug Dev. Technol. *2*, 215–224.
23. Davies, S.P., Reddy, H., Caivano, M., and Cohen, P. (2000). Specificity and mechanism of action of some commonly used protein kinase inhibitors. Biochem. J. *351*, 95–105.
24. Bain, J., McLauchlan, H., Elliott, M., and Cohen, P. (2003). The specificities of protein kinase inhibitors: an update. Biochem. J. *371*, 199–204.
25. Brehmer, D., Godl, K., Zech, B., Wissing, J., and Daub, H. (2004). Proteome-wide identification of cellular targets affected by bisindolylmaleimide-type protein kinase C inhibitors. Mol. Cell. Proteomics *3*, 490–500.
26. Godl, K., Wissing, J., Kurtenbach, A., Habenberger, P., Blencke, S., Gutbrod, H., Salassidis, K., Stein-Gerlach, M., Missio, A., Cotten, M., et al. (2003). An efficient proteomics method to identify the cellular targets of protein kinase inhibitors. Proc. Natl. Acad. Sci. USA *100*, 15434–15439.
27. Lolli, G., Thaler, F., Valsasina, B., Roletto, F., Knapp, S., Uggeri, M., Bachi, A., Matafora, V., Storici, P., Stewart, A., et al. (2003). Inhibitor affinity chromatography: profiling the specific reactivity of the proteome with immobilized molecules. Proteomics *3*, 1287–1298.
28. Knockaert, M., Gray, N., Damiens, E., Chang, Y.T., Grellier, P., Grant, K., Fergusson, D., Mottram, J., Soete, M., Dubremetz, J.F., et al. (2000). Intracellular targets of cyclin-dependent kinase inhibitors: identification by affinity chromatography using immobilised inhibitors. Chem. Biol. *7*, 411–422.
29. Wissing, J., Godl, K., Brehmer, D., Blencke, S., Weber, M., Habenberger, P., Stein-Gerlach, M., Missio, A., Cotten, M., Muller, S., et al. (2004). Chemical proteomic analysis reveals alternative modes of action for pyrido[2,3-d]pyrimidine kinase inhibitors. Mol. Cell. Proteomics *3*, 1181–1193.
30. Fabian, M.A., Biggs, W.H., Treiber, D.K., Atteridge, C.E., Azimioara, M.D., Benedetti, M.G., Carter, T.A., Ciceri, P., Edeen, P.T., Floyd, M., et al. (2005). A small molecule-kinase interaction map for clinical kinase inhibitors. Nat. Biotechnol. *23*, 329–336.
31. Manning, G., Whyte, D.B., Martinez, R., Hunter, T., and Sudarsanam, S. (2002). The protein kinase complement of the human genome. Science *298*, 1912–1934.
32. Burdine, L., and Kodadek, T. (2004). Target identification in chemical genetics: the (often) missing link. Chem. Biol. *11*, 593–597.

33. Zheng, X.S., Chan, T.F., and Zhou, H.H. (2004). Genetic and genomic approaches to identify and study the targets of bioactive small molecules. Chem. Biol. *11*, 609–618.
34. Jessani, N., and Cravatt, B.F. (2004). The development and application of methods for activity-based protein profiling. Curr. Opin. Chem. Biol. *8*, 54–59.
35. Predki, P.F. (2004). Functional protein microarrays: ripe for discovery. Curr. Opin. Chem. Biol. *8*, 8–13.
36. Kley, N., Ivanov, I., and Meier-Ewert, S. (2004). Genomics and proteomics tools for compound mode-of-action studies in drug discovery. Pharmacogenomics *5*, 395–404.
37. Kley, N. (2004). Chemical dimerizers and three-hybrid systems: scanning the proteome for targets of organic small molecules. Chem. Biol. *11*, 599–608.
38. Markwalder, J.A., Arnone, M.R., Benfield, P.A., Boisclair, M., Burton, C.R., Chang, C.H., Cox, S.S., Czerniak, P.M., Dean, C.L., Doleniak, D., et al. (2004). Synthesis and biological evaluation of 1-aryl-4,5-dihydro-1H-pyrazolo[3,4-d]pyrimidin-4-one inhibitors of cyclin-dependent kinases. J. Med. Chem. *47*, 5894–5911.
39. Wuarin, J., Buck, V., Nurse, P., and Millar, J.B. (2002). Stable association of mitotic cyclin B/Cdc2 to replication origins prevents endoreduplication. Cell *111*, 419–431.
40. Chao, S.H., Fujinaga, K., Marion, J.E., Taube, R., Sausville, E.A., Senderowicz, A.M., Peterlin, B.M., and Price, D.H. (2000). Flavopiridol inhibits P-TEFb and blocks HIV-1 replication. J. Biol. Chem. *275*, 28345–28348.
41. de Azevedo, W.F., Jr., Canduri, F., and da Silveira, N.J. (2002). Structural basis for inhibition of cyclin-dependent kinase 9 by flavopiridol. Biochem. Biophys. Res. Commun. *293*, 566–571.
42. Fry, D.W., Harvey, P.J., Keller, P.R., Elliott, W.L., Meade, M., Trachet, E., Albassam, M., Zheng, X., Leopold, W.R., Pryer, N.K., et al. (2004). Specific inhibition of cyclin-dependent kinase 4/6 by PD 0332991 and associated antitumor activity in human tumor xenografts. Mol. Cancer Ther. *3*, 1427–1438.
43. Ren, S., and Rollins, B.J. (2004). Cyclin C/cdk3 promotes Rb-dependent G0 exit. Cell *117*, 239–251.
44. Ye, X., Zhu, C., and Harper, J.W. (2001). A premature-termination mutation in the Mus musculus cyclin-dependent kinase 3 gene. Proc. Natl. Acad. Sci. USA *98*, 1682–1686.
45. Wang, D., de la Fuente, C., Deng, L., Wang, L., Zilberman, I., Eadie, C., Healey, M., Stein, D., Denny, T., Harrison, L.E., et al. (2001). Inhibition of human immunodeficiency virus type 1 transcription by chemical cyclin-dependent kinase inhibitors. J. Virol. *75*, 7266–7279.
46. Rarey, M., Kramer, B., Lengauer, T., and Klebe, G. (1996). A fast flexible docking method using an incremental construction algorithm. J. Mol. Biol. *261*, 470–489.
47. Nugiel, D.A., Vidwans, A., Etzkorn, A.M., Rossi, K.A., Benfield, P.A., Burton, C.R., Cox, S., Doleniak, D., and Seitz, S.P. (2002). Synthesis and evaluation of indenopyrazoles as cyclin-dependent kinase inhibitors. 2. Probing the indeno ring substituent pattern. J. Med. Chem. *45*, 5224–5232.
48. Skehan, P., Storeng, R., Scudiero, D., Monks, A., McMahon, J., Vistica, D., Warren, J.T., Bokesch, H., Kenney, S., and Boyd, M.R. (1990). New colorimetric cytotoxicity assay for anticancer-drug screening. J. Natl. Cancer Inst. *82*, 1107–1112.
49. Kaiser, C., Michaelis, S., and Mitchell, A. (1994). Methods in Yeast Genentics (Cold Spring Harbor, NY: Cold Spring Harbor Laboratory Press).
50. Romero, F., Dargemont, C., Pozo, F., Reeves, W.H., Camonis, J., Gisselbrecht, S., and Fischer, S. (1996). p95vav associates with the nuclear protein Ku-70. Mol. Cell. Biol. *16*, 37–44.